Supporting information

Preparation of Fluorescein-Based Chemosensors and Their Sensing Behaviors toward Silver Ions

Chang Liu [a], Shanshan Huang [a], Huirong Yao [a], Song He [a], Yan Lu [a], Liancheng Zhao[a,b] and Xianshun Zeng[a,*]

a. Key Laboratory of Display Materials & Photoelectric Devices, Ministry of Education, School of Materials Science & Engineering, Tianjin University of Technology, Tianjin 300384, China

b. School of Materials Science and Engineering, Institute of Information Functional Materials& Devices, Harbin Institute of Technology, Harbin 150001, China.

Fax: +86 22 60 21 52 26; Email: xhzeng@tjut.edu.cn

1 Materials and instruments

All cations in the form of nitrate salts, all anions in the form of sodium salts were purchased from Sigma-Aldrich Chemical Company and used without further purification. All other chemicals used were local products of analytical grade. All solvents (analytical grade and spectroscopic grade) were obtained commercially and used as received unless otherwise mentioned. NMR spectra were recorded on a Bruker spectrometer at 400 (^{1}H NMR) MHz and 100 (^{13}C NMR) MHz. Chemical shifts (δ values) were reported in ppm down field from internal Me_4Si (^{1}H and ^{13}C NMR). High-resolution mass spectra (HRMS) were acquired on an Agilent 6510 Q-TOF LC/MS instrument (Agilent Technologies, Palo Alto, CA) equipped with an electrospray ionization (ESI) source. Elemental analyses were performed on a Vanio-EL elemental analyzer (Analysensystem GmbH, Germany). UV absorption spectra were recorded on a Shimadzu UV-2550 UV-VIS spectrophotometer. Fluorescence measurements were performed using a Hitachi F-4600 fluorescence spectrophotometer and a quartz cell (1 cm × 1 cm). Melting points were recorded on a Boethius Block apparatus and are uncorrected.

2 General spectroscopic methods

The general spectroscopic methods have been described previously. All cations and anions were dissolved in deionised water to obtain 10 mM stock solutions. The chemosensors **L1** and **L2** were dissolved in DMF to obtain 10 mM stock solutions. Before spectroscopic measurements, the solution was freshly prepared by diluting the stock high concentration

solution to the required concentration. All of the experiments were conducted at standard barometric pressure and room temperature.

3 Determination of quantum yields

Fluorescence quantum yields of **L1**, **L2**, **L1**/$(Ag^{+})_2$ and **L1**/$(Ag^{+})_2$ complex were determined in ethanol solutions by using fluorescein solution (Φ_f = 0.95, 0.1 M NaOH) as references. The concentrations of fluorescein, ligands and complexes were 1×10^{-6} M. The quantum yields[S1] were calculated using Eq.1:

$$\Phi_u = [(A_s F_u n^2)/ (A_u F_s n_0^2)]\Phi_s \qquad \text{(Eq.1)}$$

Where A_s and A_u are the absorbance of the reference and sample solution at the reference excitation wavelength (463 nm), F_s and F_u are the corresponding integrated fluorescence, n and n_0 are the refractive indexes of the solvents for the sample (1.362 for ethanol) and reference (1.333 for water) solutions.

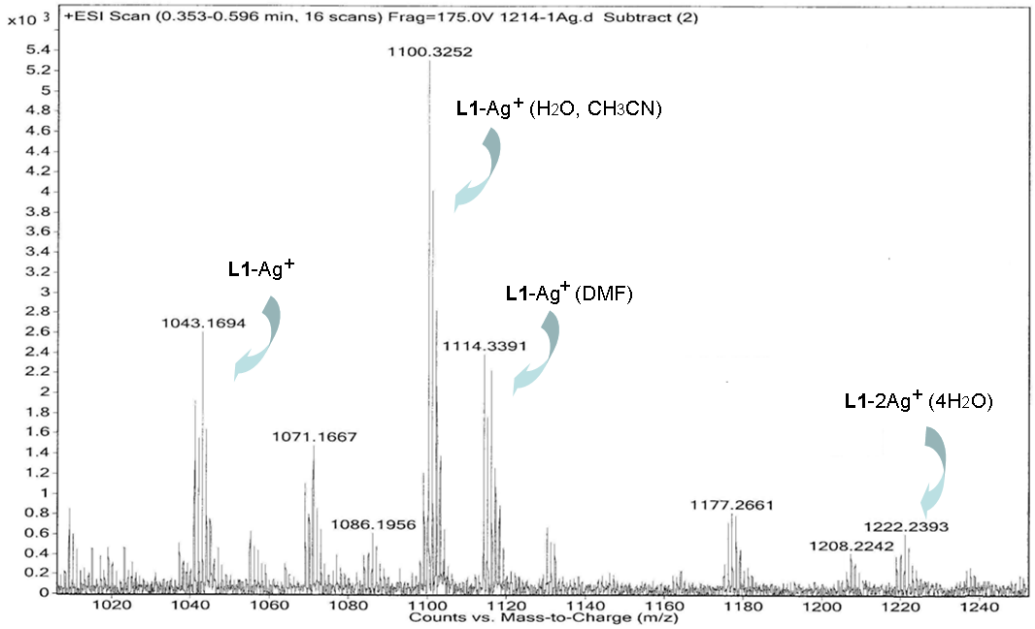

Figure S1. HRMS spectra of the reaction mixture of **L1** with one equivalent of Ag^{+} ions. A series of peaks at *m*/*z* = 1043.1694 (**L1**·Ag^{+}, form **B**), *m*/*z* = 1100.3252 (**L1**·Ag^{+}(H_2O, CH_3CN), form **A**), and *m*/*z* = 1114.3391 (**L1**·Ag^{+}(DMF), form **A**) corresponding to the 1:1 complex of **L1** and Ag^{+} ions were observed. Only a weak peak at *m*/*z* =1222.2393 (**L1**·2Ag^{+}(4H_2O)) corresponding to the 1:2 complex of **L1** and Ag^{+} ions was observed.

[S1] X. Yang, Z. T. Pan and Y. Ma, *J. Anal. Sci*., 2003, **19**, 588.

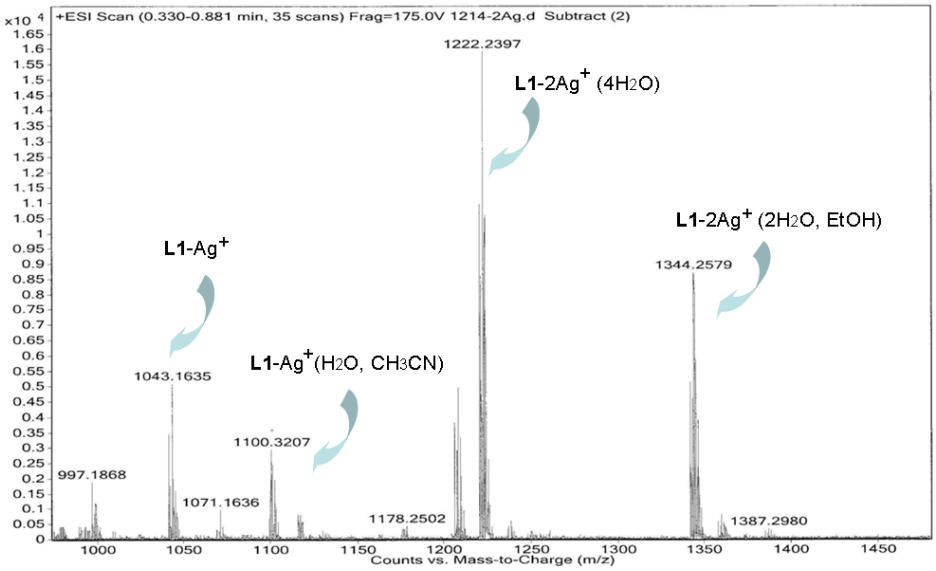

Figure S2. HRMS spectra of the reaction mixture of **L1** with two equivalents of Ag^+ ions. The main peaks at *m/z* =1222.2393 (**L1**·2Ag^+(4H_2O)) and *m/z* =1344.2579 (**L1**·2Ag^+(2H_2O, EtOH)) corresponding to the 1:2 complex of **L1** and Ag^+ ions were observed. Weak peaks at *m/z* = 1043.1694 (**L1**·Ag^+, form **B**), *m/z* = 1100.3252 (**L1**·Ag^+(H_2O, CH_3CN) , form **A**) corresponding to the 1:1 complex of **L1** and Ag^+ ions was also observed.

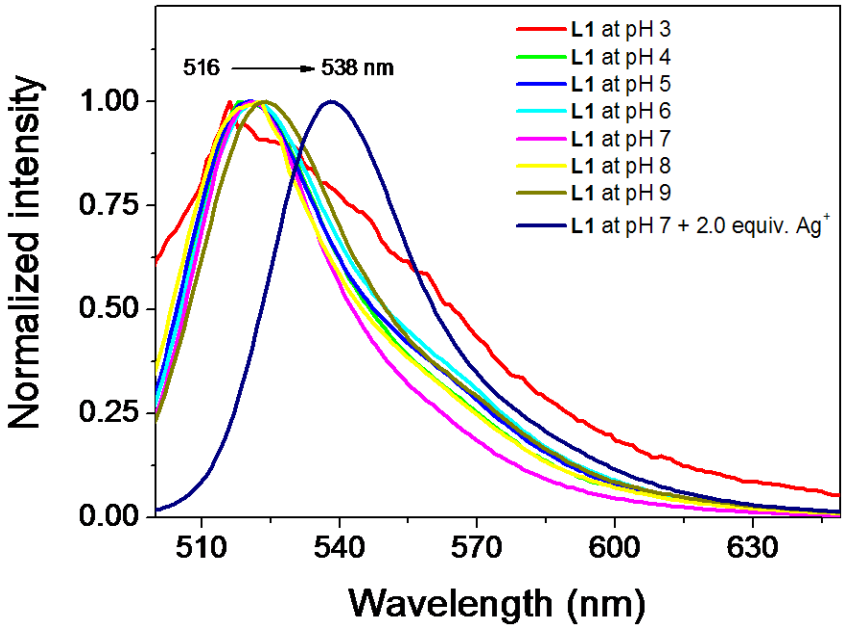

Figure S3. Normalized fluorescence spectra of the chemosensors **L1** (1.0 μM) in EtOH/H_2O (1:1, v/v) at different pH. pH 3: λ_{em} = 516 nm; pH 4: λ_{em} = 518 nm; pH 5: λ_{em} = 520 nm; pH 6: λ_{em} = 521 nm; pH 7: λ_{em} = 521 nm; pH 8: λ_{em} = 522 nm; pH 9: λ_{em} = 523 nm. Upon addition of 2.0 equivalents Ag^+ ion to a solution of **L1** at pH 7, the emission maxmum is red shift to λ_{em} = 538 nm. (λ_{ex} = 463 nm; slit: 5 nm.)

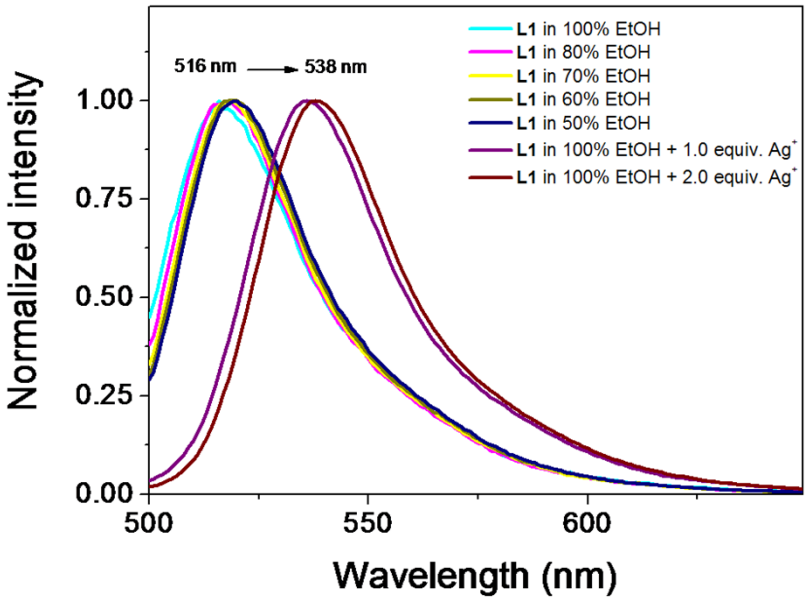

Figure S4. Normalized fluorescence spectra of the chemosensors **L1** (1.0 μM) in different ratio of EtOH/H_2O. In 100% EtOH: λ_{em} = 516 nm; In 80% EtOH: λ_{em} = 518 nm; In 70% EtOH: λ_{em} = 520 nm; In 60% EtOH:λ_{em} = 521 nm; In 50% EtOH: λ_{em} = 522 nm. Upon addition of 1.0 equivalents Ag^+ ion to a solution of **L1**, the emission maximum is red shift to λ_{em} = 536 nm. Upon addition of 2.0 equivalents Ag^+ ion to a solution of **L1**, the emission maximum is red shift to λ_{em} = 538 nm. (λ_{ex} = 463 nm; slit: 5 nm.)

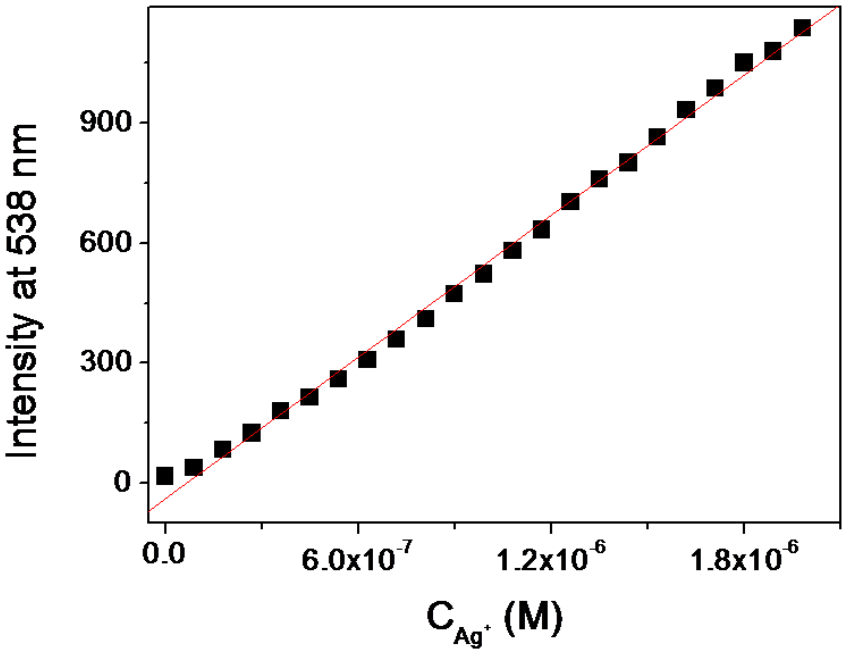

Figure S5. The fluorescence enhancement of **L1** (1.0 μM) were linearly related to the concentrations of Ag^+ ions when the ratio of [Ag^+]/[**L1**] is below to 2 : 1 (0-1.98 equivalents). Linear regression equation: y = -38.0078 + 5.8834 × 10^8 x, R = 0.9983.

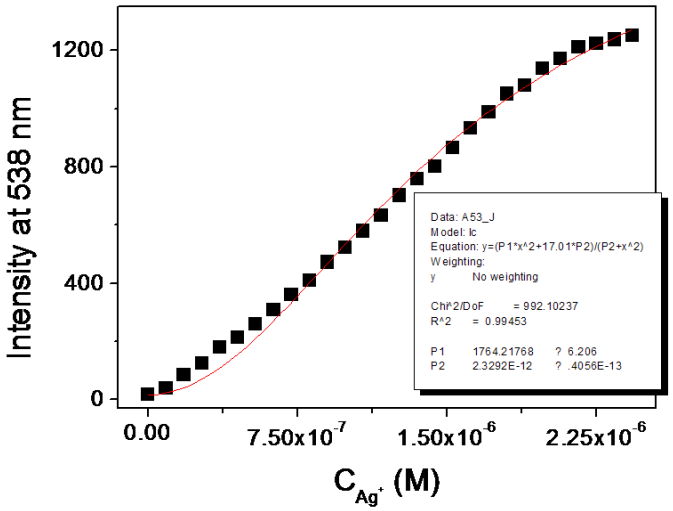

Figure S6. A nonlinear least-square analysis of a 1:2 complex of **L1** (1.0 μM) and Ag^+ cation (0 - 2.43 equivalents). The nonlinear curve fitness based on 1:2 complex expression: [S2]

$$F = (F_{max}[X]^n + F_{min}K_d)/(K_d + [X]^n)$$

where F_{max} and F_{min} are the fluorescence intensity of **L1** in the presence and absence of Ag^+, [X] are the concentrations of Ag^+; *n* represents the number of silver ions bound per probe. The dissociation constant K_d was deduced to be 2.3292×10^{-12} M (with correlation coefficient R = 0.9945).

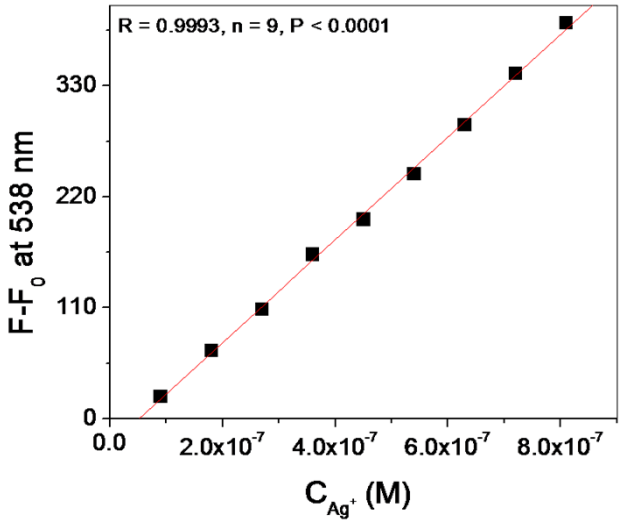

Figure S7. Emission (at 538 nm) of **L1** (1.0 μM) at different concentrations of silver ions (0, 0.09, 0.18, 0.27, 0.36, 0.45, 0.54, 0.63, 0.72, 0.81 μM) added. A good linear relationship between the fluorescence intensity and the Ag^+ concentration could be obtained in the 0-0.81 μM concentration range (R = 0.9993). The detection limit was then calculated with the equation: detection limit = $3\sigma_{bi}/m$,[S3] where σ_{bi} is the standard deviation of blank measurements (σ_{bi} = 0.7104, derived from nine measurements), m (5.0975 x 10^8) is the slope between intensity *versus* sample concentration. The detection limit was measured to be 4×10^{-9} M. λ_{ex} = 463 nm, Slit: 5.0 nm.

[S2] E. Cielen, A. Stobiecka, A. Tahri, G. J. Hoornaert, F. C. De Schryver, J. Gallay, M. Vincent and N. Boens, *J. Chem. Soc., Perkin Trans.*, 2002, **2**, 1197.
[S3] L. Wang, W. Qin, X. Tang, W. Dou, W. Liu, Q. Teng and X. Yao, *Org. Biomol. Chem.*, 2010, **8**, 3751

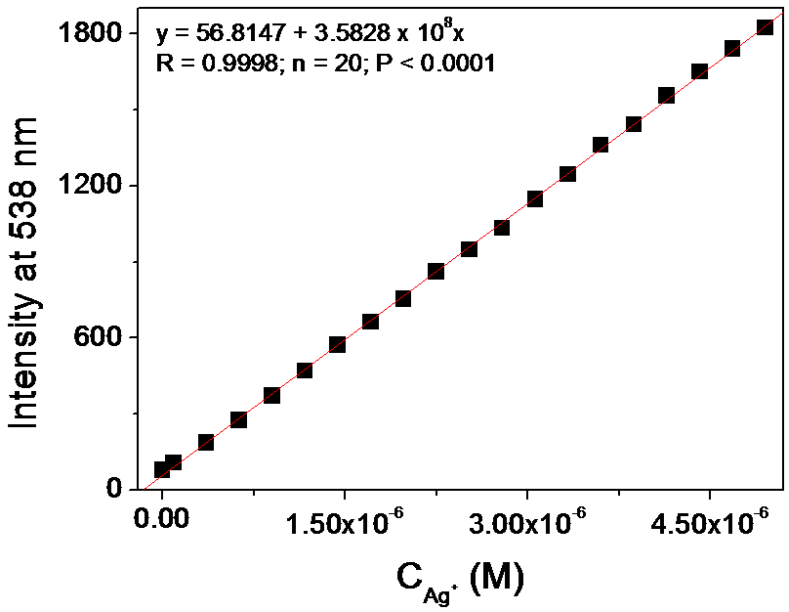

Figure S8. The fluorescence enhancement of **L2** (1.0 μM) were linearly related to the concentrations of Ag^+ ions when the ratio of $[Ag^+]/[\mathbf{L2}]$ is below to 5 : 1 (0- 4.95 equivalents). Linear regression equation: $y = 56.8147 + 3.5828 \times 10^8$ x, $R = 0.9998$.

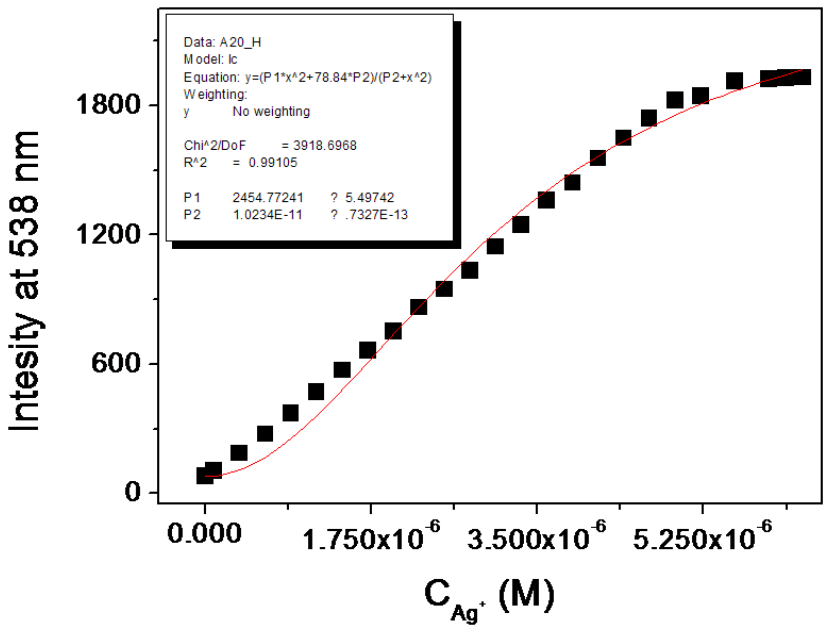

Figure S9. Curve of fluorescence emission intensities of **L2** versus increasing concentration of Ag^+. A nonlinear least-square analysis of a 1:2 complex of **L2** (1.0 μM) and Ag^+ cation (0 – 6.3 equivalents).[S2] The dissociation constant K_d was deduced to be 1.0234×10^{-11} M (correlation coefficient $R = 0.9911$).

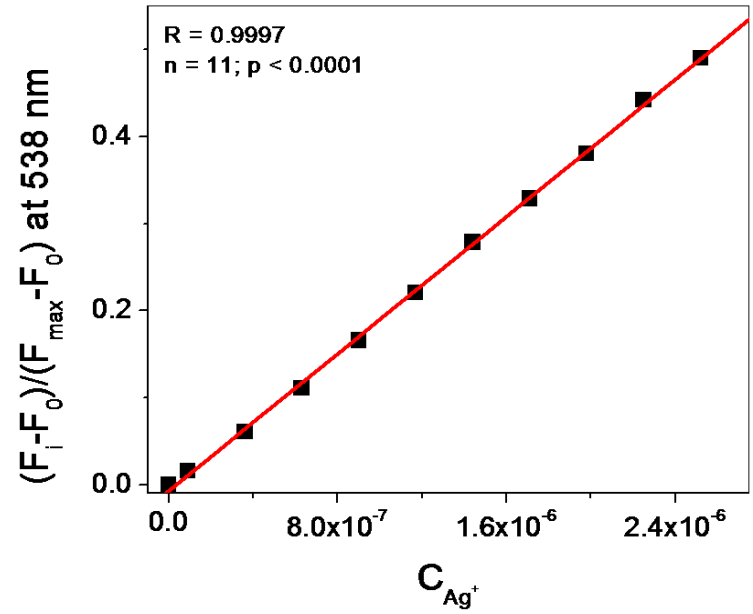

Figure S10. Detection limit of **L2** (1.0 μM) toward Ag^+. Emission (at 538 nm) of **L2** at different concentrations of Ag^+ (0, 0.09, 0.38, 0.63, 0.9, 1.17, 1.44, 1.71, 1.98, 2.25, 2.52 μM) added, normalized between the minimum emission (0.0 μM Ag^+) and the emission at 2.52 μM Ag^+. The detection limit was determined to be 3×10^{-8} M.[S4]

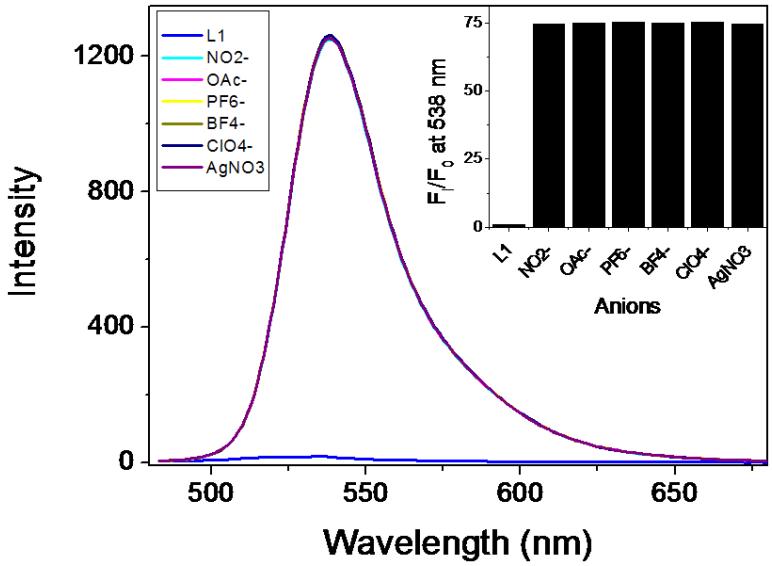

Figure S11. Fluorescence changes of **L1** with Ag^+ salts with different counteranions. Inset: Histogram representing the fluorescence enhancement and quenching of **L1** (1.0 μM) with Ag^+ salts (2.0 μM) in the presence of different counteranions (ClO_4^-, NO_2^-, PF_6^-, AcO^- and BF_4^-). For the entire test, excitation and emission were performed at 463 and 538 nm. (λ_{ex} = 463 nm; slit: 5.0 nm).

[S4] M. Shortreed, R. Kopelman, M. Kuhn and B. Hoyland, *Anal. Chem*. 1996, **68**, 1414

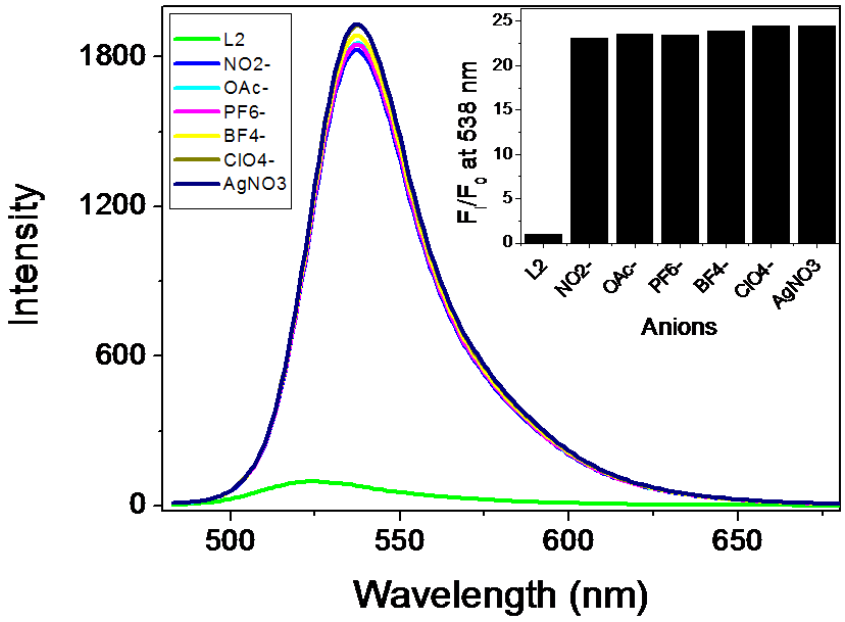

Figure S12. Fluorescence changes of **L2** (1.0 μM) with 2.0 equivalents of Ag^+ salts with different counteranions. Inset: Histogram representing the fluorescence enhancement and quenching of **L2** with Ag^+ salts in the presence of different counteranions (ClO_4^-, NO_2^-, PF_6^-, AcO^- and BF_4^-). For the entire test, excitation and emission were performed at 463 and 538 nm. (λ_{ex} = 463 nm; slit: 5 nm).

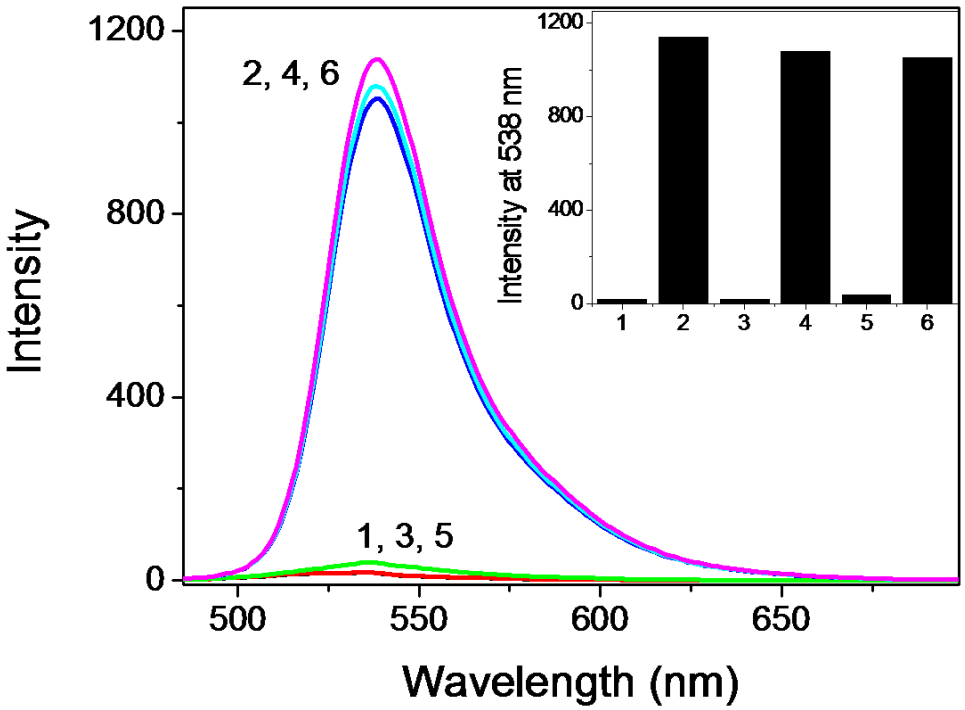

Figure S13. The fluorescence spectra of **L1** (1.0 μM) upon the addition of 2.0 μM $AgNO_3$ in ethanol. Na_2S (1.0 μM) was added to **L1** + Ag^+ mixture to show the reversible binding nature of Ag^+ with **L1**. 1: **L1**; 2: **L1** + Ag^+; 3: **L1** + Ag^+ + S^{2-}; 4: **L1** + Ag^+ + S^{2-} + Ag^+; 5: **L1** + Ag^+ + S^{2-} + Ag^+ + S^{2-}; 6: **L1** + Ag^+ + S^{2-} + Ag^+ + S^{2-} + Ag^+.

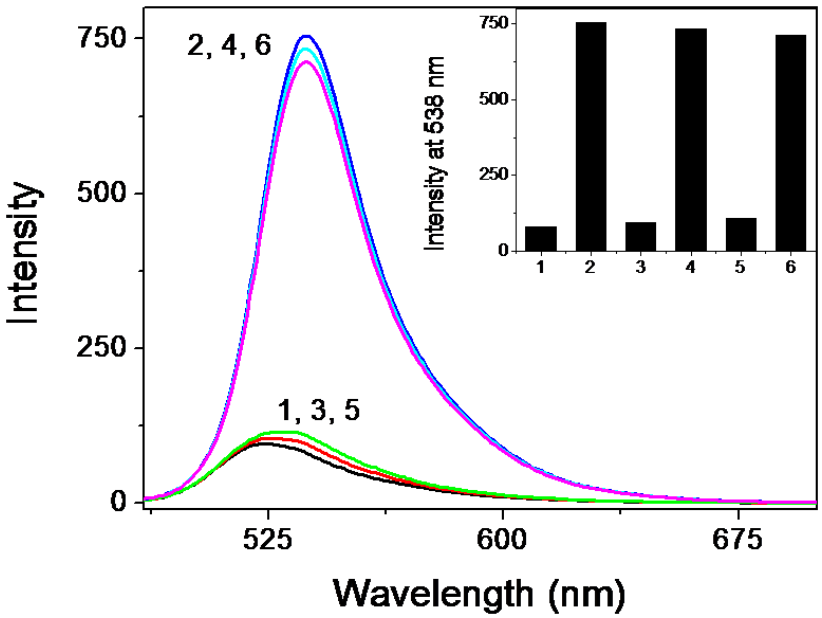

Figure S14. The fluorescence spectra of **L2** (1.0 μM) upon the addition of 2.0 μM $AgNO_3$ in ethanol. Na_2S (1.0 μM) was added to **L2** + Ag^+ mixture to show the reversible binding nature of Ag^+ with **L2**. 1: **L2**; 2: **L2** + Ag^+; 3: **L2** + Ag^+ + S^{2-}; 4: **L2** + Ag^+ + S^{2-} + Ag^+; 5: **L2** + Ag^+ + S^{2-} + Ag^+ + S^{2-}; 6: **L2** + Ag^+ + S^{2-} + Ag^+ + S^{2-} + Ag^+.

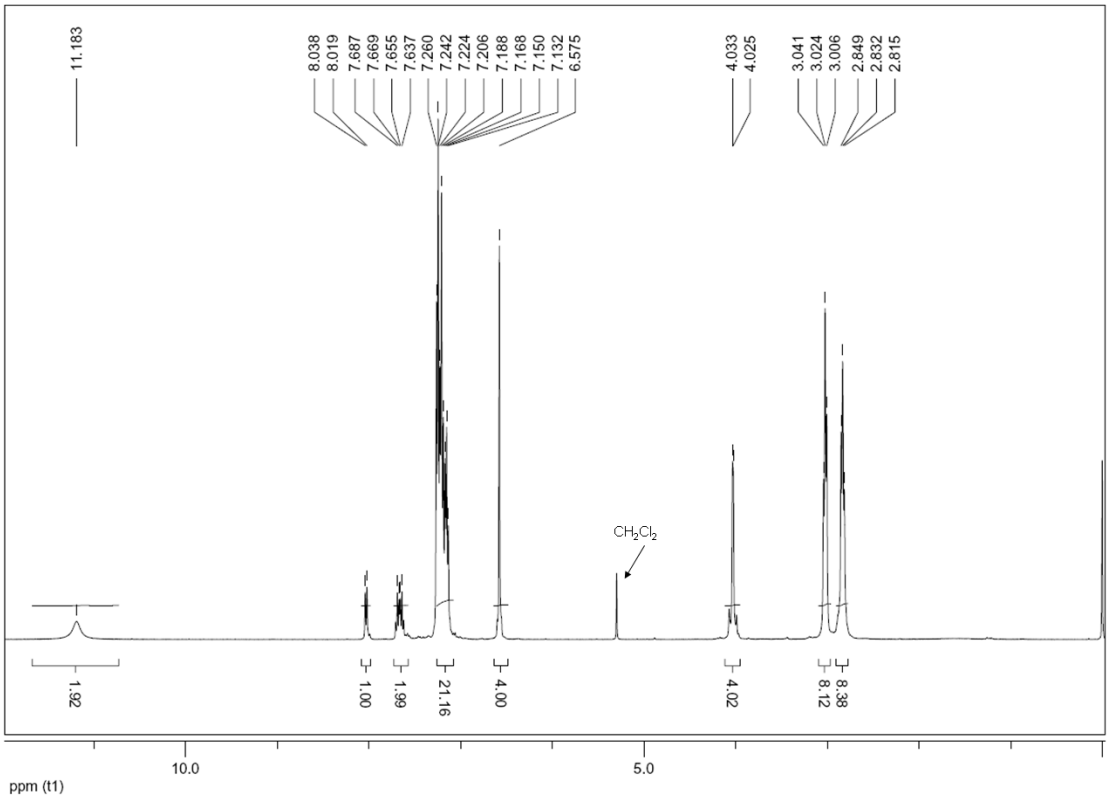

Figure S15. ^1H NMR of the chemosensor **L1** (400 MHz, $CDCl_3$).

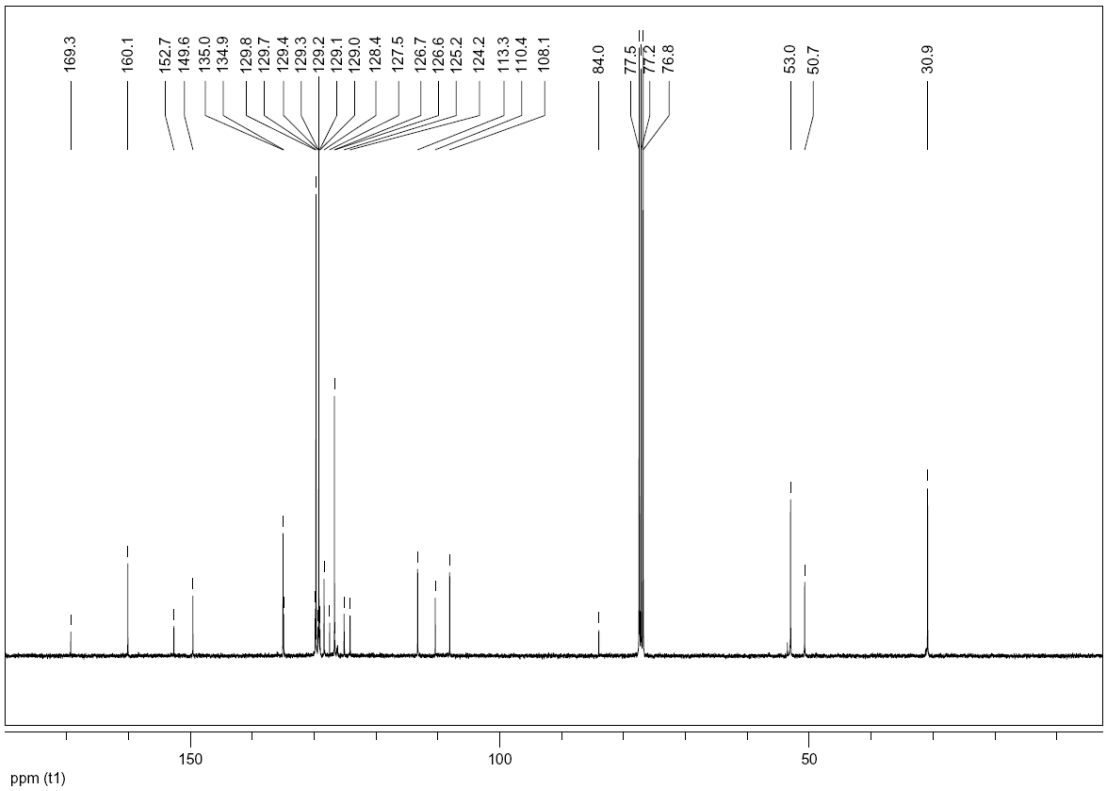

Figure S16. ^{13}C NMR of the chemosensor **L1** (100 MHz, $CDCl_3$).

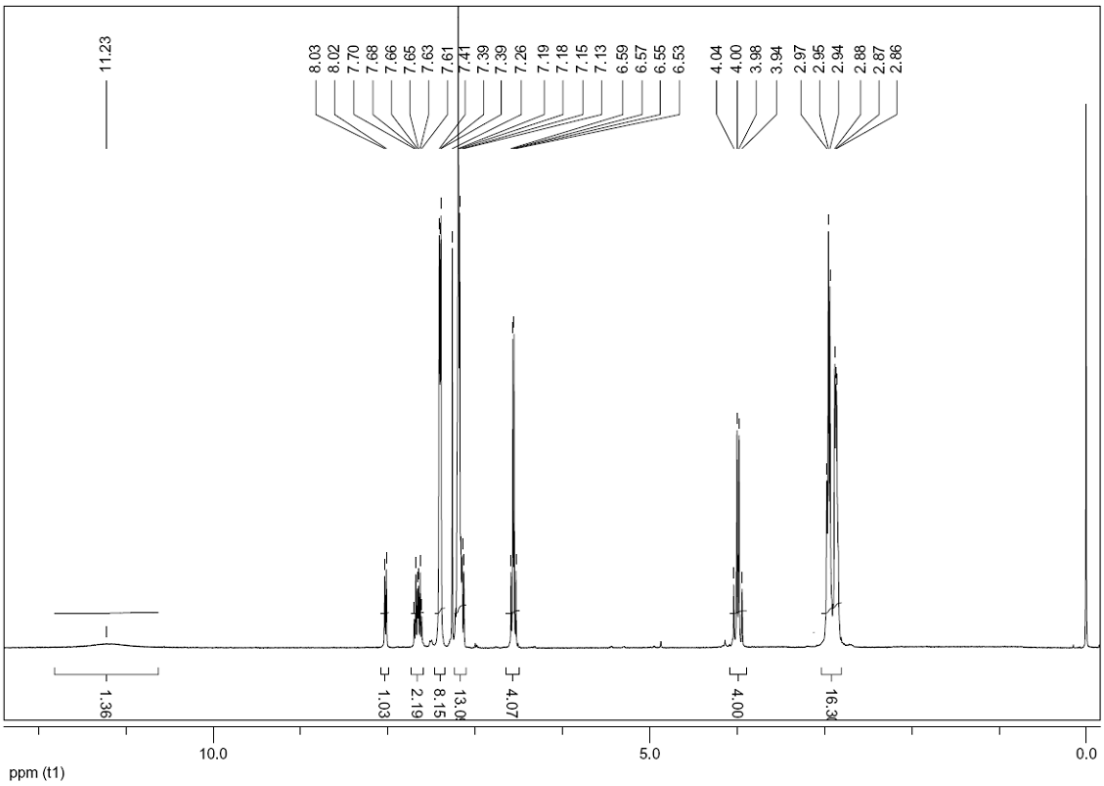

Figure S17. ^{1}H NMR of the chemosensor **L2** (400 MHz, $CDCl_3$).

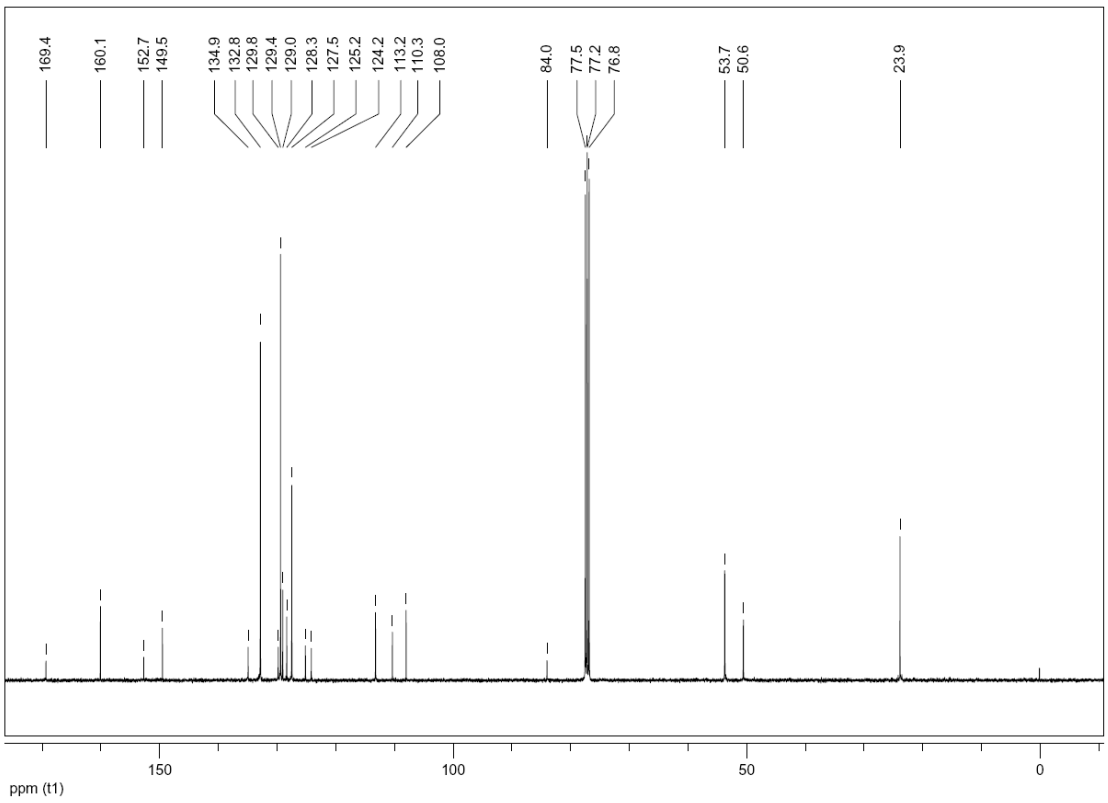

Figure S18. ^{13}C NMR of the chemosensor **L2** (100 MHz, $CDCl_3$).